The MSS Control Point Location Error Filter

for Landsat-D.*

I. Levine

General Electric Company Space Division

4701 Forbes Blvd., Lanham, MD   20801

ABSTRACT

The theory and results of modeling for the MSS Control Point Location Error Filter are presented. The filter produces the maximum-likelihood estimates for average values of the spacecraft position and attitude errors during a single scene. The quality of the filter performance is characterized by the maximal cross and along-track residual errors for which probability distributions can be calculated analytically for a given pattern of control points. The filter with an automatic selection of the best set of estimates provides geodetic correction at 90% of pixels with residual errors less than 40m for four or more control points and the mean-squared measurement errors of the order of 20-25m. The same accuracy can be preserved for eight or more control points and measurement errors of 30-35m.

INTRODUCTION

The ground control points (CP), whose locations are measured on systematically corrected imagery and whose true coordinates are known from maps, give highly precise information on image displacements at each of the CP's. The differences between true and measured locations provide the input to a filter, which produces refined estimates of the spacecraft ephemeris and attitude errors. Then these estimates are used for geodetic correction.

The MSS filter theory, represented in Section I, is based on

1) presentation of image distortions, expressed in Local Space Oblique Mercator coordinates, as a linear function of deviations in spacecraft attitudes and position (Ref.1), and

2) recognition of the fact, that MSS processing is limited to a single scene with no more than 20 CP's. It is unlikely that any filter can assess the true time dependence in the deviations during a single scene. But we still believe that in some cases the MSS filter will be able to produce an reliable estimate of average rates.   L.

An accuracy of these estimates is discussed in Section 2. The covariance analysis of the estimate errors shows that image distortions caused by the roll and cross-track deviations are so similar that their origins can be determined only by near perfect measurements. Thus, the filter is unable to produce an reliable estimate of both deviations. At the same time, the filter can provide an equivalent estimate for either variable, say, roll, which compensates distortions due to both sources. Analogously, for the pitch and along-track deviations. The analysis of covariances shows also, that initial uncertainties in rates may be reduced only for the equivalent roll + cross-track and pitch + along-track rates if there are more than 15 CP's and the mean-squared measurement errors are of the order of 10-15m. So, in cases of few CP's, that is of interest to us, only four estimates should be taken into consideration: for the yaw, radial and equivalent pitch and roll deviations.

Section 3 introduces three global characteristics of filter performance: the maximal cross and along-track residual errors, together with combined error in distance. These characteristics can be obtained analytically and they establish upper levels of errors for any given configuration of CP's. The final formulae for probability distributions are presented; more details may be found in Ref.2. It is known that pattern, which CP's form on imagery, have a strong effect on filter performance. Examples, given in Section 4, show that one of the most important simple characteristics of CP's distribution is the maximal cross-track separation, which has been defined as the maximum of the cross-track distances between every pair of CP's.

The examples demonstrate also, that for every pattern of CP's, measurement errors, and initial uncertainties in deviations, there is an optimal set of estimates, minimizing the residual errors. An approximate algorithm, providing the automatic selection of such a set, is described in Section 5. Results of modeling indicate that the MSS filter with the automatic selection provides the 90% average errors less than .5 pixel (40m) for 4 or more CP's and the mean-squared measurement errors of the order of 20-25m, or for 8 or more CP's and measurement errors of 30-35m.

I.   THE MSS FILTER EQUATIONS

Ref. [1] shows that the local SOM coordinates of a frame point, $\overline{X} = (X_1, X_2)$, may be represented as

$$\overline{X} = \overline{X}_o + \mu\overline{\delta}, \tag{1}$$

where $\overline{X}_o$ is true coordinates of the point, $\overline{\delta} = (\delta_1, \delta_2, \ldots, \delta_\ell)$ is a vector of the spacecraft position and attitude deviations, and μ is a $(2 \times \ell)$ matrix of the partial derivatives (PD), computed at the same point. Now let $\overline{Z} = (Z_1, Z_2)$ be the coordinates of a CP obtained from a map. We will assume that

$$\overline{Z} = \overline{X}_o + \overline{\xi}, \tag{2}$$

where $\overline{\xi} = (\xi_1, \xi_2)$ is a vector of Gaussian measurement errors with zero expectation values and the covariance matrix R.

From (1) and (2), it follows that the measured at a CP displacement,

$$\overline{\Delta X} = \overline{X} - \overline{Z} = \mu\overline{\delta} - \overline{\xi} , \qquad (3)$$

is also normally distributed with

$$E(\overline{\Delta X}) = E(\mu\overline{\delta}) - E(\overline{\xi}) = \mu\overline{\delta}$$

$$cov(\overline{\Delta X}) = E(\overline{\xi}\overline{\xi}^T) = R$$

Thus, the conditional probability density for $\overline{\Delta X}$ can be written as

$$P = (\overline{\Delta X}/\overline{\delta}) = const \cdot exp \left[-\tfrac{1}{2}(\overline{\Delta X} + \mu\overline{\delta})^T R^{-1}(\overline{\Delta X} + \mu\overline{\delta}) \right]$$

Let us assume that $\overline{\delta}$ is constant during a scene. Then a joint density of displacements at N control point is

$$P(\overline{\Delta X}^1, \overline{\Delta X}^2, \ldots, \overline{\Delta X}^N/\overline{\delta}) = const \cdot \prod_{k=1}^{N} exp(-\tfrac{1}{2} (\overline{\Delta X}^k -$$

$$- \mu^k\overline{\delta})^T R^{-1}(\overline{\Delta X}^k - \mu^k\overline{\delta})) ,$$

where upper index k indicates $\overline{\Delta X}$ and μ associated with the k-th CP.

It is known, that the maximum likelihood estimate of $\overline{\delta}$ (we will denote it as $\hat{\delta}$) is a solution of equation

$$\nabla L (\overline{\delta}) = 0 , \qquad (4)$$

where

$$L(\overline{\delta}) = \ln P = -\tfrac{1}{2} \sum_{k=1}^{N} (\overline{\Delta X}^k - \mu^k\overline{\delta})^T R^{-1}(\overline{\Delta X}^k - \mu^k\overline{\delta}), \qquad (5)$$

and differential operator ∇ is defined in Appendix.

It is known also that

$$E(\hat{\delta}) = \overline{\delta} \qquad (6)$$

and in our case (Gaussian conditional density) the covariance matrix of $\hat{\delta}$ is

$$cov(\delta) = E((\hat{\delta}-\overline{\delta})(\hat{\delta}-\overline{\delta})^T) = - (\nabla L(\overline{\delta})_\nabla^T)^{-1} \qquad (7)$$

Note from here the summation index k will be omitted. Eq. (4) and (5) yield

$$\nabla L = -\tfrac{1}{2} \sum \nabla(\overline{\Delta X} - \mu\overline{\delta})^T R^{-1} (\overline{\Delta X} - \mu\overline{\delta}) =$$

$$= \tfrac{1}{2} \sum \mu^T R^{-1}(\overline{\Delta X} - \mu\overline{\delta}) = 0 \qquad (8)$$

and thus, the solution $\hat{\delta}$ can be written as

$$\hat{\delta} = M_o^{-1} Y_o \; , \tag{9}$$

where

$$M_o = \sum \mu^T R^{-1} \mu$$

$$Y_o = \sum \mu^T R^{-1} \overline{\Delta X}$$

Noting that

$$\nabla L \nabla^T = - \sum \mu^T R^{-1} \mu = - M_o$$

we also have from (7) that

$$\text{cov}(\delta) = M_o^{-1} \tag{10}$$

Now let ξ_1, ξ_2 be independent with the dispersions σ_1^2, σ_2^2. In that case

$$R = \begin{pmatrix} \sigma_1^2 & 0 \\ & \\ 0 & \sigma_2^2 \end{pmatrix}$$

and (9) and (10) yield

$$\hat{\delta} = M^{-1} Y \tag{11}$$

$$\text{cov}(\hat{\delta}) = \sigma_1^2 M^{-1} \; , \tag{12}$$

where M, Y are matrices with elements

$$m_{ij} = \sum (\mu_{1i} \mu_{1j} + \frac{\sigma_1^2}{\sigma_2^2} \mu_{2i} \mu_{2j}) \tag{13}$$

$$y_i = \sum (\mu_{1i} \Delta X_1 + \frac{\sigma_1^2}{\sigma_2^2} \mu_{2i} \Delta X_2) \tag{14}$$

Elements of the matrix M^{-1} will be denoted as m_{ij}^{-1} , i.e. $M^{-1} = (m_{ij}^{-1})$.

Once $\hat{\delta}$ is determined, it can be used for geodetic correction. With geodetically corrected coordinates of a point being $\overline{X} + \mu\hat{\delta}$, the residual error at the point, $\overline{\varepsilon} = (\varepsilon_1, \varepsilon_2)$, can be written as

$$\overline{\varepsilon} = \overline{X} + \mu\hat{\delta} - \overline{X}_o = \overline{X} + \mu\hat{\delta} - (\overline{X} + \mu\overline{\delta}) =$$

$$= \mu(\hat{\delta} - \overline{\delta}) \tag{15}$$

Thus, $\bar{\varepsilon}$ is normally distributed with zero mean and the covariance matrix

$$\text{cov}(\bar{\varepsilon}) = E\left\{\mu(\hat{\delta}-\bar{\delta})\left[\mu(\hat{\delta}-\bar{\delta})\right]^T\right\} =$$
$$= \mu\, E\left\{(\delta-\bar{\delta})(\delta-\bar{\delta})^T\right\}\mu^T = \sigma_1^2\,\mu\, M^{-1}\mu^T \qquad (16)$$

Eq (16) defines local two-dimensional distribution of the residual errors at a given frame point. It can be used also for detection of 'outliers', i.e. bad measurements at CP's. From (3) it follows, that after geodetic correction, the measured displacement at the k-th CP's, $\bar{\varepsilon}_k$, can be expressed as

$$\bar{\varepsilon}_k = \overline{\Delta X} - \mu\hat{\bar{\delta}} = \mu(\bar{\delta}-\hat{\bar{\delta}}) + \bar{\xi}$$

As a sum of two independent Gaussian variables, $\bar{\varepsilon}_k$ also is Gaussian with zero mean and the covariance matrix.

$$\text{cov}(\bar{\varepsilon}_k) = \sigma_1^2\,\mu\, M^{-1}\,\mu^T + R = Q \qquad (17)$$

The two-dimensional probability density for $\bar{\varepsilon}_k$ is represented by the countour ellipses

$$\Phi(\bar{e}) = \bar{e}^T\, Q^{-1}\,\bar{e} = \text{const} = \lambda^2$$

It is well-known, that the probability that the 'point' $\bar{\varepsilon}_k$ is inside the countour ellipse is $\chi^2(\lambda^2)$, so the k-th CP should be treated as an outlier if

$$\Phi(\bar{\varepsilon}_k) > \lambda^2 \, ,$$

where λ^2 corresponds to a chosen confidence level. For instance, $\lambda^2 = 9.21$ for the 99% confidence level.

All derived above formulae can be easily generalized to include the case when $\bar{\delta}$ is a slow-changing function of time. Introducing the average deviations and rates during a scene,

$$\bar{\alpha} = (\alpha_1, \alpha_2, \ldots \alpha_\ell) \text{ and } \bar{\beta} = (\beta_1, \beta_2, \ldots \beta_\ell),$$

we can approximate the deviation at time t as

$$\bar{\delta} = \bar{\alpha} + \bar{\beta}t \qquad (18)$$

Now the displacement at the k-th CP at time t^k is

$$\overline{\Delta X}^k = \mu^k(\bar{\alpha} + \bar{\beta}t^k) + \bar{\xi}$$

and the maximum likelihood function of $\bar{\alpha}$, $\bar{\beta}$ can be written as

$$L(\bar{\alpha},\bar{\beta}) = -\tfrac{1}{2} \sum_{k=1}^{N} (\Delta \bar{X}^k - \mu^k(\bar{\alpha} + \bar{\beta}t^k)) R^{-1}$$

$$(\Delta \bar{X}^k - \mu^k(\bar{\alpha} - \bar{\beta}t^k))^T.$$

From the above, one can obtain that the estimates of $\bar{\alpha}$ and $\bar{\beta}$ (denoted as $\hat{\alpha}$ and $\hat{\beta}$) are given by

$$\begin{vmatrix} \hat{\alpha} \\ \hat{\beta} \end{vmatrix} = M_1^{-1} \begin{vmatrix} Y \\ Y' \end{vmatrix} , \tag{19}$$

where Y is given by (14) and components of Y' are

$$y'_i = \sum (\mu_{1i} \Delta X_1 + \frac{\sigma_1^2}{\sigma_2^2} \mu_{2i} \Delta X_2)t \tag{20}$$

The matrix M_1 consists of four submatrices

$$M_1 = \begin{vmatrix} M & M' \\ M' & M'' \end{vmatrix} ,$$

where M is defined by (13) and elements of M' and M'', m'_{ij} and m''_{ij} , are

$$m'_{ij} = \sum (\mu_{1i}\mu_{1j} + \frac{\sigma_1^2}{\sigma_2^2} \mu_{2i} \mu_{2j})t \tag{21}$$

$$m''_{ij} = \sum (\mu_{1i}\mu_{1j} + \frac{\sigma_1^2}{\sigma_2^2} \mu_{2i} \mu_{2j})t^2 \tag{22}$$

We have also that $E(\hat{\alpha}) = \bar{\alpha}$, $R(\hat{\beta}) = \bar{\beta}$, and

$$cov(\hat{\alpha},\hat{\beta}) = \sigma_1^2 M_1^{-1} \tag{23}$$

Introducing the estimate of deviation at time t, $\hat{\delta} = \hat{\alpha} + \hat{\beta}t$, we have that

$$E(\hat{\delta}) = E(\hat{\alpha}) + t \cdot E(\hat{\beta}) = \bar{\alpha} + \bar{\beta}t = \bar{\delta}$$

and the covariance matrix of $\hat{\delta}$ is

$$\text{cov}(\hat{\delta}) = E((\hat{\alpha} - \bar{\alpha})(\hat{\alpha} - \bar{\alpha})^T) + 2 t E((\hat{\alpha} - \bar{\alpha})(\hat{\beta} - \bar{\beta})^T) +$$

$$+ t^2 E((\hat{\beta} - \bar{\beta})(\hat{\beta} - \bar{\beta})^T) =$$

$$= C + 2tC' + t^2C'', \tag{24}$$

where C, C' and C'' are the $\ell \times \ell$ submatrices of M_1^{-1}

$$M_1^{-1} = \begin{vmatrix} C & C' \\ C' & C'' \end{vmatrix} \tag{25}$$

Further it will be considered that the filter can estimate, at the most, the along-track (AT), cross-track (CT), and radial (RAD) position deviations and rates, together with deviations and rates in the pitch (P), roll (R) and yaw (Y). σ_1 and σ_2 will correspond to the cross-track and along-track measurements.

II. COVARIANCE ANALYSIS

The covariance matrices, $\text{cov}(\hat{\delta})$ and $\text{cov}(\hat{\alpha},\hat{\beta})$, completely characterize an accuracy of estimates, which can be achieved by the filter for a given configuration of CP's and the mean-squared measurement errors σ_1 and σ_2. It is well-known, that a pattern, which CP's form on imagery, has a strong effect on filter performance, especially for a small number of CP's. At the same time, our calculations show that for $N \geq 10$ elements of the covariance matrices insignificantly depend upon a distribution of CP's. For $\sigma_1 \approx \sigma_2$ the standard deviation of the estimates are approximately proportional to $\sigma_1 N^{-\frac{1}{2}}$. At the present time, σ_1 and σ_2 are not expected to be less than 10 and 12m, respectively; the MSS filter will be processing up to 20 CP's per scene.

Table I shows the standard deviations of $\hat{\delta}$ computed for $\sigma_1 = 10$, $\sigma_2 = 12$m and 50 (randomly located in a frame) CP's. Comparison of the standard deviations with initial uncertainties in the spacecraft position and orientation, given in Table 2, demonstrates complete inefficiency of the filter in that case. The reason is simple: PD with respect to the R and CT deviations, as well as PD with respect to P and AT, are almost linearly dependent. As a result, the matrix M is nearly singular, and thus Eq. (9) can not give a reliable value of $\hat{\delta}$. In other words, distortions, caused by the R and CT (or P and AT) deviations, are so similar that the difference would be revealed only in near perfect imagery by near perfect measurements.

It prompts not to estimate CT and AP deviations at all, considering the corresponding image distoritons as a result of additional fictitious deviations in R and P, respectively. Thus, the filter should be treated as a source of appropriate geodetic corrections, rather than true estimates.

The covariance analysis for time-dependent deviations shows that the filter is unable to produce reliable estimates of the Y and RAD rates even for $N = 50$: the standard deviations of the estimates are 4-5 times as much as their initial uncertainties.

At the same time, the filter provides mediocre estimates for combined R + CT and P + AT rates when $N = 15 - 20$ and σ_1, σ_2 are of the order of 10-15m. Table 3 shows such an example for $N = 20$, $\sigma_1 = 10$, and $\sigma_2 = 12m$. Note, that initial uncertainties in the R + CT and P + AT rates are .83 and .82 μrad/sec (these values have been computed by data from Table 2).

Despite the fact, that in some favorable conditions the filter can cope with these rates, such a case will not be considered below. Being interested chiefly in the case of few CP's we will take into account only estimates of the P,R,Y and RAD deviations.

III.   THE MAXIMAL RESIDUAL ERRORS

The current requirements to geometric correction accuracy are specified in terms of .5 pixel 90% of the time. Accordingly, we will evaluate the filter performance by the 90% guantile of probability distribution, computed for the residual errors which were observed at points of some, say 15x15, grid for randomly distributed deviations, measurement errors, and possibly, CP's locations. Three types of the 90% errors may be introduced on two-dimensional grids: for the CT and AT components of the residuals errors and for the total residual displacements $\bar{\varepsilon} = (\varepsilon_1^2 + \varepsilon_2^2)^{\frac{1}{2}}$. The last characteristic will be referred to as DIST.

It should be noted, that actually all these characteristics can be obtained only by stochastic modeling. At the same time there are two additional global characteristics, which can be computed relatively simply: probability distributions of the maximal CT and AT errors. These distributions describe errors at the worst frame points and thus establish the upper level of possible errors for given CP's.

Let us introduce the error in the j-th estimate, $\Delta_j = \delta_j - \hat{\delta}_j$. Now, Eq. (15) may be rewritten as

$$\varepsilon_1 = \sum \mu_{1j} \Delta_j$$

$$\varepsilon_2 = \sum \mu_{2j} \Delta_j \qquad (j = 1,2,3,4)$$

It is known that all PD increase towards the corner points of a frame. The CT and AT errors also reach maximal magnitudes at a corner point [1], although it is never known beforehand at what specific point. At the corner points only four PD, namely, $\mu_{21}, \mu_{12}, \mu_{23}$, and μ_{14}, have significant values. Moreover, with an error less than .1%, they may be replaced with their maximum values, μ_{ij}^m (retaining, of course, correct sign). Thus, at the corner points

$$\varepsilon_1 \approx \mu_{12}^m \Delta_2 + \mu_{14}^m \Delta_4$$

$$\varepsilon_2 \approx \mu_{21}^m \Delta_1 + \mu_{23}^m \Delta_3$$

Noting that μ_{23} and μ_{14}, PD with respect to Y and RAD, have opposite signs at the ends of every scan line, we always can find a corner point, where $\mu_{12} \Delta_2$ and $\mu_{14} \Delta_4$ have the same sign (analogously, for $\mu_{21}\Delta_1$ and $\mu_{23} \Delta_3$). Being indifferent to signs of ε_1 and ε_2, we finally have that the maximal (absolute) CT and AT errors, γ_1 and γ_2, are

$$\gamma_1 = |\mu_{12}\,\Delta_2| + |\mu_{14}\,\Delta_4|$$
$$\gamma_2 = |\mu_{21}\,\Delta_1| + |\mu_{23}\,\Delta_3| \tag{26}$$

Here we have omitted the superscript m.

Fortunately, Δ_2, Δ_4 and Δ_1, Δ_3 are practically independent and thus these expressions may be used separately to derive corresponding distribution and moments (Ref.2).

The following are the final formulae for mean value and variance of γ_i:

$$E(\gamma_i) = \sqrt{\frac{2}{\pi}}\,(S_1 + S_2) \tag{27}$$

$$\mathrm{Var}(\gamma_i) = (1 - \frac{2}{\pi})\,(S_1^2 + S_2^2) +$$

$$+ \frac{4}{\pi}\,S_1\,S_2 \cdot (\rho \cdot \arccos(r) + r - 1)\,, \tag{28}$$

where

$$\left.\begin{aligned}
r &= (1 - \rho^2)^{\frac{1}{2}} \\[4pt]
S_1^2 &= \sigma_1^2\,\mu_{12}\,m_{22}^{-1} \\[4pt]
S_2^2 &= \sigma_2^2\,\mu_{14}\,m_{44}^{-1} \\[4pt]
\rho &= \frac{|m_{24}^{-1}|}{\sqrt{m_{22}^{-1} \cdot m_{44}^{-1}}}
\end{aligned}\right\} \quad \text{for } i = 1$$

$$\left.\begin{aligned}
S_1^2 &= \sigma_1^2\,\mu_{21}^2\,m_{11}^{-1} \\[4pt]
S_2^2 &= \sigma_2^2\,\mu_{23}^2\,m_{33}^{-1} \\[4pt]
\rho &= \frac{|m_{13}^{-1}|}{\sqrt{m_{11}^{-1} \cdot m_{33}^{-1}}}
\end{aligned}\right\} \quad \text{for } i = 2$$

The probability distribution of γ_i can be written as

$$\Pr(\gamma_i < A) = \frac{A\,2^{\frac{1}{2}}}{S_1\,\pi^{\frac{1}{2}}} \int_0^1 \exp(-\frac{A^2 t}{2S_1^2}) \times$$

$$\left[\, F(B(n + \rho \cdot t - n \cdot t) + F(B \cdot (n - \rho \cdot t - n \cdot t)) - 1 \,\right] dt,$$

where $n = \dfrac{S_1}{S_2}$, $B = \dfrac{A}{S_1 \cdot r}$,

$$F(u) = \frac{1}{\sqrt{2\pi}} \int_{-\infty}^{u} \exp(-t^2/2) \, dt,$$

and S_1, S_2, ρ are given by (29).

For a given value of error, A, the corresponding probability can be easily computed by means of standard subroutines. Modeling has shown an excellent coincidence of theoretical and empirical values of $E(\gamma_1)$ and $Var(\gamma_1)$. Smirnov's Test also demonstrates sufficient coincidence of theoretical and empirical distributions.

Eq. (26) may be used also for evaluation of the maximal residual error in distance, which we define as

$$d_m = (\gamma_1^2 + \gamma_2^2)^{\frac{1}{2}}$$

We could not derive an exact distribution for d_m. But we have noticed that empirical distribution of d_m^2 are similar to Gamma-distribution with the same means and variances. Because $E(d_m^2)$ and $Var(d_m^2)$ can be obtained analytically, we have decided to approximate distribution of d_m^2 by Gamma-distribution, which is written here as

$$Pr(A) = \frac{1}{b^a \Gamma(a)} \int_0^A u^{a-1} \exp\left(-\frac{u}{b}\right) \cdot du$$

where

$$a = \frac{E(d_m^2)^2}{Var(d_m^2)} \tag{30}$$

$$b = \frac{Var(d_m^2)}{E(d_m^2)} \tag{31}$$

Because, γ_1 and γ_2 are practically independent,

$$E(d_m^2) = E(\gamma_1^2) + E(\gamma_2^2) \tag{32}$$

$$Var(d_m^2) = Var(\gamma_1^2) + Var(\gamma_2^2) \tag{33}$$

In Ref.2 it is shown that

$$E(\gamma_1^2) = s_1^2 + s_2^2 + \frac{4s_1 s_2}{\pi} (\rho \arccos(r) + r) \tag{34}$$

and

$$\mathrm{Var}(\gamma_i^2) = 2(S_1^2 + S_2^2)^2 + 24S_1^2 S_2^2 \rho \quad +$$

$$+ \; \frac{32}{\pi} (S_1^2 + S_2^2) S_1 S_2 (r + \rho \arccos(r)) \; -$$

$$- \; \frac{32 \; S_1^2 \; S_2^2}{\pi 2} \; (\; r + \rho \arccos(r))^2 \tag{35}$$

Here S_1^2, S_2^2 and ρ are given by (29). Eq. (30)-(35) yield a and b, which are used to compute a probability $\mathrm{Pr}(A) = \mathrm{Pr}(A^2)$ for any A by means of a standard subroutine for Gamma-distribution. Smirnov's Test shows sufficient coincidence of the approximations and empirical distributions for d_m; differences between values of errors for corresponding probabilities are less than 5-7%.

IV. EXAMPLES

Table 4 presents means, the standard deviations, and the 90% errors for the maximal CT and AT errors, together with the 90% errors in distance (DIST). These data have been obtained by modeling (M) and analytically (T) for $\sigma_1 = \sigma_2 = 10m$ and initial uncertainties given in Table 2 (except example 9, where AT = 185m, CT = 35m, RAD = 65m, P = R = 120 μrad, and Y = 35 μrad).

From 300 to 600 samples have been used to establish results for each case. The examples correspond to five selected configurations of CP's, depicted in Fig.1. Table 5 describes the examples and shows the mean-squared errors of estimates. Examples 1-3 and 7-8 illustrate the fact that for given configuration of CP's, measurement errors, and initial uncertainties, there is an optimal set of estimates, which provides minimum errors. For distribution A, that set includes P and R for distribution C it includes P,R, and Y. Examples 8 and 9 demonstrate also that such a set depends upon initial errors in deviations.

As we already know, the partial derivatives μ_{12}, μ_{14}, μ_{21}, and μ_{23} represent the main effects of the position and attitude deviations on image distortions. At the same time, there is significant distinction between μ_{12}, μ_{21} and μ_{14}, μ_{23}: when the former are almost constant in a frame, the second increase their magnitudes along every scan line. Thus, up to the second order effects, P and R estimates do not depend upon position of CP's in a scene. Roughly speaking, they depend upon average CT and AT displacements at all CP's. On the contrary, to detect effects of the Y and RAD deviations, we should observe differences of these displacements, so the bigger the CT distances between CP's, the bigger differences in corresponding μ_{14} and μ_{23}, and the higher an accuracy of the Y and RAD estimates. Thus, a simple but important characteristic of CP's distribution is the maximal cross-track separation, H, which we define as the maximum of cross-track distances between every pair of CP's.

Example 1 shows that for small cross-track separations (H=29.7 km) the Y and RAD estimates are absolutely insufficient (457 μrad and 292 m) and, as a result, the residual errors are large even for very modest measurement errors. On the other hand, even smaller number of CP's may lead to better results if they are 'nicely' separated (example 4 for N = 2 and H = 169 km). Comparasion of examples 4 and 5 shows that an along-track shift of CP's does not affect significantly an accuracy of results if cros-track positions are preserved. In addition, example 6

suggests that a shift of CP's as a whole in the cross-track direction towards to the frame bounds increases errors. It implies that it is always desirable to have CP's placed symmetrically along the track.

Analyzing results of modeling, we have noted that the 90% CT and AT errors can be approximated as

$$\gamma_i = E(\gamma_i) + 1.5 \sqrt{Var(\gamma_i)} \tag{36}$$

where $E(\gamma_i)$ and $Var(\gamma_i)$ are given by (27) and (28). We have no explanation of that fact, but it was verified on a large number of cases which have shown that an error of such an approximation usually does not exceed 5%.

V. AUTOMATIC SELECTION OF ESTIMATES

As it has been shown, for every pattern of CP's, measurement errors and initial uncertainties, there is an optimal set of estimates which reduces the residual errors. Consequently, the filter's performance can be improved if it will automatically select an appropriate set of estimates. Our approximate algorithm of selection is based on the fact that γ_1 and γ_2 are practically independent, and, bigger maximal errors almost always lead to bigger average errors. In our specific case, the a priori known uncertainties in P + AT and R + CT are always bigger than errors of corresponding estimates (at least, for mean-squared measurement errors less than 40m). Thus, these estimates always ought to be included in an optimal set. Now, all we need is to compute γ_1 twice, with and without the use of the RAD estimate. In the second case, the standard deviation of the RAD estimate must be replaced with the initial mean-squared error. Analogously γ_2 should be computed twice to determine when the Y estimates ought to be employed.

Table 6 presents the 90% CT, AT, and DIST errors, computed on a 15x15 grid as a function of σ_1 for various number of CP's.* Results for each case have been established by 300-500 randomly generated sets of CP, measurement errors and deviations. CP's were generated so that the distances between every pair of them were not less than 75 km for $N \leqslant 4$, 50 km for $N = 5,6$ and 25 km for $N \geqslant 7$. Additional restriction forbad generation of CP's on the frame borders. The 90% DIST errors also depicted in Fig.2.

As one can see, the filter provides geodetic correction with the 90% errors less than 40m if $\sigma_1 \leqslant 20m$ and $N \geqslant 4$. For $\sigma_1 = 30$ m only 8 or more CP's can guarantee that accuracy. Note these results do not include errors due to neglected uncertainties in rates. These additional errors, accumulated during 15 sec (i.e. with respect to the frame center) can be evaluated as 8.6 m (σ) in either direction. Being relatively small, they do not affect significantly the total errors.

It should be pointed out, that the automatic selection only slightly reduces the average residual errors. At the same time, it essentially moderates errors in relatively rare cases of extremely bad distributions of CP's.

---

* Note, that the CT and AT errors are Gaussian and thus may be described also by the corresponding standard deviations.

REFERENCES

1. I. Levine, "Computational Aspects of Geometric Correction Data Generation in the Landsat-D Imagery Processing", The sixth annual Flight Mechanics/ Estimation Theory Symposium, NASA/Goddard Space Flight Center, October 27/28 1981.

2. I. Levine, "The MSS Control Point Location Error Filter: General Theory and Results of Modeling", GE 1T81-LSD-LAS-102, 3/6/81.

APPENDIX

$\bar{a}$ - ℓ x 1 matrix (vector)

$\bar{a}^T = (a_1, a_2, \ldots, a_\ell)$ - transposed vector $\bar{a}$

$E(\bar{a})$ - mathematical expectation of $\bar{a}$

$cov(\bar{a}) = E((\bar{a} - E(\bar{a}))(\bar{a} - E(\bar{a}))^T)$ - covariance matrix of $\bar{a}$

$Var(b)$ - variance of b.

$$\nabla = \left(\frac{\partial}{\partial \delta_1}, \frac{\partial}{\partial \delta_2}, \ldots \frac{\partial}{\partial \delta_\ell} \right)$$ symbolic differential

operator defined for $U = (u_1, u_2, \ldots, u_\ell)$ as

$$\nabla U^T = \begin{vmatrix} \dfrac{\partial u_1}{\partial \delta_1} & \cdots & \dfrac{\partial u_\ell}{\partial \delta_1} \\ \cdots\cdots\cdots \\ \cdots\cdots\cdots \\ \dfrac{\partial u_1}{\partial \delta_\ell} & \cdots & \dfrac{\partial u_\ell}{\partial \delta_\ell} \end{vmatrix}$$

If A is a ℓ x ℓ matrix,

$$\nabla(\bar{\delta}^T A \bar{\delta}) \nabla^T = 2A$$

Table 1

Mean-squared errors in estimates

$(N = 50, \sigma_1 = 10, \sigma_2 = 12)$

P μrad	R μrad	Y μrad	AT m	CT m	RAD m
2591	34	375	2059	299	20

Table 2

Initial uncertainties in deviations and rates (1σ)

	P,R,Y	AT	CT	RAD
deviations	350 μrad	550m	110m	37m
rates	.81 μrad/sec	.16m/sec	.065m/sec	.65m/sec

Table 3

Mean-squared errors in estimates.

$(N = 20, \sigma_1 = 10m, \sigma_2 = 12m)$

deviations				rates	
R + CT μrad	P + AT μrad	Y μrad	RAD m	R + CT μrad/sec	P + AT μrad/sec
3.3	4.0	52.2	31.1	.5	.6

Table 4

The 90% maximal CT, AT, and DIST errors (in meters)

error			Example								
			1	2	3	4	5	6	7	8	9
γ_1 (CT)	mean	M	38.3	9.4	9.7	12.6	13.3	57.1	11.0	5.5	10.9
		T	38.1	8.6	8.6	12.2	12.2	55.6	11.0	5.3	11.0
	STD	M	26.0	4.6	4.8	6.6	6.7	40.3	6.1	3.2	5.7
		T	26.8	4.6	4.6	6.6	6.6	41.6	6.1	3.2	6.1
	90%	M	72.9	16.0	15.7	21.5	22.4	113.8	19.4	10.0	18.5
		T	75.9	14.8	14.8	21.2	21.2	115.0	19.3	9.6	19.3
γ_2 (AT)	mean	M	45.8	42.7	30.0	12.9	12.2	64.5	11.8	11.2	7.3
		T	42.1	42.0	30.7	12.3	12.2	61.0	10.9	10.9	6.5
	STD	M	30.3	30.7	20.4	6.7	6.5	44.4	6.0	6.2	3.5
		T	29.9	29.9	2.0	6.6	6.6	45.7	6.1	6.1	3.6
	90%	M	88.0	85.9	59.0	22.0	21.0	124.5	20.0	19.6	12.0
		T	84.3	84.2	57.9	21.2	21.1	126.7	19.3	18.9	11.3
d_m (DIST)	90%	M	110.0	86.4	60.2	27.3	27.8	154.8	24.6	20.6	20.3
		T	105.5	85.5	61.2	26.5	28.9	156.7	26.2	21.5	22.1

Table 5

Description of Examples in Table 4.

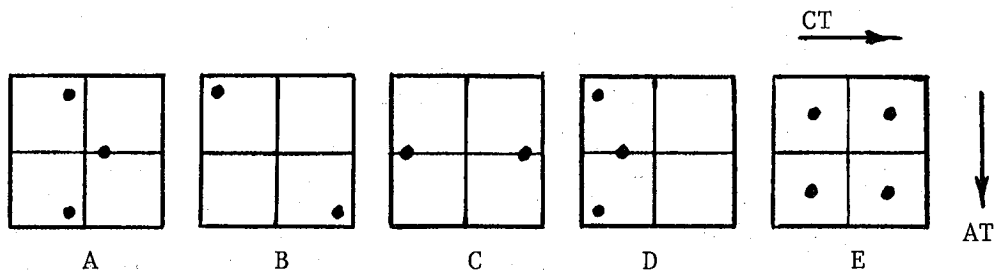| Example	N	distribution (See Fig.1)	H (km)	mean-squared errors in estimates			
				P (μrad)	R (μrad)	Y (μrad)	RAD (m)
1	3	A	29.7	14	13	457	292
2	3	A	29.7	14	8	457	–
3	3	A	29.7	8	8	–	–
4	2	B	169.0	10	10	87	63
5	2	C	160.4	10	10	88	63
6	3	D	29.5	47	42	461	298
7	4	E	112.9	7	7	93	66
8	4	E	112.9	7	7	93	–
9	4	E	112.9	7	7	–	66

Figure 1. Control Point Distributions

Table 6

The 90% CT, AT, and DIST errors (in meters) as a function of N and σ_1

$$(\sigma_2 = 1.2\ \sigma_1).$$

| N	$\sigma_1 = 10m$			$\sigma_1 = 20m$			$\sigma_1 = 30m$			$\sigma_1 = 40m$		
	CT	AT	DIST	CT	AT	DIST	CT	AT	DIST	CT	AT	DIST
1	19.0	51.5	53.1	33.4	59.9	65.7	49.5	73.3	81.6	68.1	87.4	104.
2	13.4	31.5	33.0	24.2	47.0	49.7	34.9	57.4	63.0	49.0	65.1	74.4
3	10.8	20.6	22.1	19.8	38.8	40.8	28.4	47.5	52.0	38.2	58.5	65.3
4	10.0	16.5	18.3	17.6	31.1	33.7	25.0	45.9	49.4	33.9	51.2	57.3
5	9.5	14.4	16.2	16.5	29.9	32.4	23.4	43.4	46.4	32.5	49.8	55.1
6	9.0	13.8	14.9	14.7	26.6	28.6	20.8	39.6	42.5	28.3	49.2	53.3
8	9.0	12.9	14.4	13.6	23.5	25.3	18.5	35.1	37.4	24.7	43.0	47.1
10	8.3	11.0	13.0	12.2	22.5	24.1	17.8	30.6	33.3	22.1	42.3	45.2
15	7.8	8.8	9.9	9.9	16.3	18.1	14.2	24.4	26.5	16.9	33.4	35.2
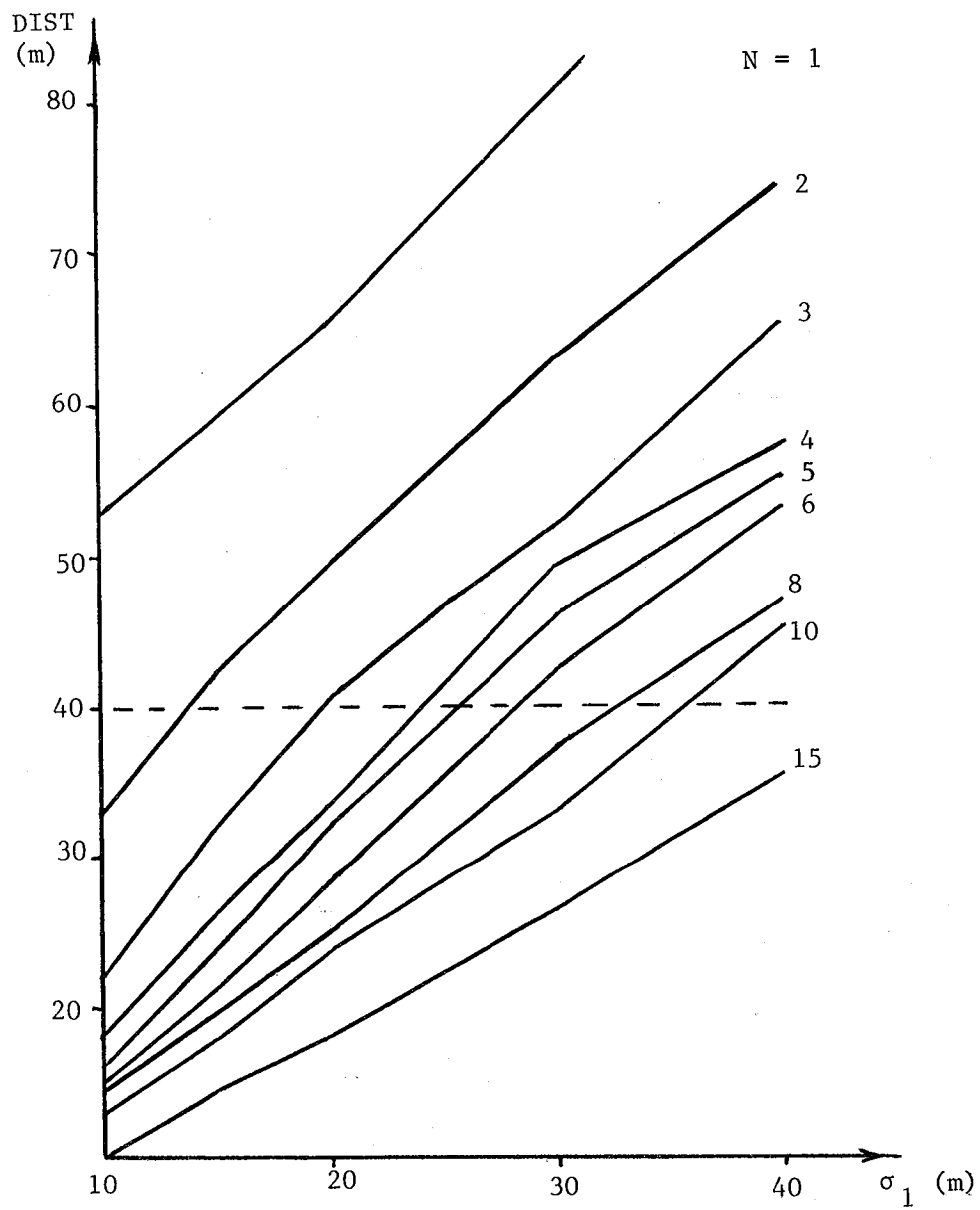
Figure 2.

90% errors in distance as a function of measurement errors ($\sigma_2 = 1.2\sigma_1$).